REPORT DOCUMENTATION PAGE

Form Approved
OMB No. 0704-0188

1. REPORT DATE *(DD-MM-YYYY)*	2. REPORT TYPE	3. DATES COVERED *(From – To*
17-Feb-2005	Journal Article	Jan 2003 – Feb 2004

4. TITLE AND SUBTITLE

Gain and Loss in an Optically Pumped Mid-Infrared Laser

5a. CONTRACT NUMBER

5b. GRANT NUMBER

5c. PROGRAM ELEMENT NUMBER

6. AUTHOR(S)

A. Ongstad, R. Kaspi, C. Moller, M. Tilton, J. Chavez, G. Dente

5d. PROJECT NUMBER
4866

5e. TASK NUMBER
LY

5f. WORK UNIT NUMBER
12

7. PERFORMING ORGANIZATION NAME(S) AND ADDRESS(ES)

8. PERFORMING ORGANIZATION REPORT NUMBER

9. SPONSORING / MONITORING AGENCY NAME(S) AND ADDRESS(ES)

AFRL/DELS
3550 Aberdeen Ave SE
Kirtland AFB NM 87117-5776

10. SPONSOR/MONITOR'S ACRONYM(S)

11. SPONSOR/MONITOR'S REPORT NUMBER(S)

12. DISTRIBUTION / AVAILABILITY STATEMENT
Approved for public release; distribution is unlimited.

13. SUPPLEMENTARY NOTES
Published in J. Appl. Phys. 95(21), 1619, 2004

14. ABSTRACT

We report on measurements of the temperature dependence of the gain and internal waveguide loss of a 3.4 μm, optically pumped InAs/InGaSb, type II, W laser. A high-resolution Fourier Transform Infrared (FTIR) spectrometer was used to measure the laser mode spectra below threshold. To obtain an accurate determination of the gain, a full curve fit to the spectral output of the Fabry-Perot cavity was utilized. Our results indicate very low waveguide loss at 78 K, with no apparent increase up to at least 120 K. Additional measurements of the gain properties of the device reveal a rapidly decreasing differential gain, dG/dP and a rapidly increasing transparency pump power with increasing temperature. Moreover, measurements of the peak gain at a constant pumping show a rapid decline with increasing temperature. Theoretical superlattice empirical pseudopotential model (SEPM)-based calculations suggest that the substantial differences between the conduction and valence subband in-plane curvatures contribute to the rapid decline in gain with increasing temperature.

15. SUBJECT TERMS
W laser, InAs/InGaSb, gain, waveguide loss, empirical pseudopotential modeling

16. SECURITY CLASSIFICATION OF:			17. LIMITATION OF ABSTRACT	18. NUMBER OF PAGES	19a. NAME OF RESPONSIBLE PERSON
a. REPORT	b. ABSTRACT	c. THIS PAGE			Dr. Andrew Ongstad
Unclassified	Unclassified	Unclassified	Unlimited	24	19b. TELEPHONE NUMBER *(include area code)* (505) 853-3207

Gain and Loss in an Optically Pumped Mid-Infrared Laser

A. P. Ongstad, R. Kaspi , and C. M. Moeller,
Air Force Research Laboratory, Directed Energy Directorate, Kirtland AFB, Albuquerque, NM 87117

M. L. Tilton, J. R. Chavez
Boeing Defense and Space Group, Albuquerque, New Mexico 87106

G. C. Dente
GCD Associates, Albuquerque, New Mexico 87110

Abstract

We report on measurements of the temperature dependence of the gain and internal waveguide loss of a 3.4 μm, optically pumped InAs/InGaSb, type II, W laser. A high-resolution Fourier Transform Infrared (FTIR) spectrometer was used to measure the laser mode spectra below threshold. To obtain an accurate determination of the gain, a full curve fit to the spectral output of the Fabry-Perot cavity was utilized. Our results indicate very low waveguide loss ($a \approx 2$ cm^{-1}) at 78 K, with no apparent increase up to at least 120 K. Additional measurements of the gain properties of the device reveal a rapidly decreasing differential gain, dG/dP and a rapidly increasing transparency pump power with increasing temperature. Moreover, measurements of the peak gain at constant pumping show a rapid decline with increasing temperature. Theoretical superlattice empirical pseudopotential model (SEPM)-based calculations suggest that the substantial differences between the conduction and valence subband in-plane curvatures contribute to the rapid decline in gain with increasing temperature.

Introduction

The recent introduction of the mid-IR W-integrated absorber (W-IA) lasers based on InAs/InGaSb/InAs type-II quantum wells has allowed for considerable improvements in the output power and beam quality of optically pumped lasers.[1-4] The W-IA epitaxy is formed by placing type-II quantum wells between thick InGaAsSb quaternary layers which are specifically designed to absorb the pump radiation. The quaternary layers are lattice matched to the GaSb substrate. While the W active region per period is quite thin (< 100 A), the much thicker (≥ 1000 A) IA layer per period allows for a large fraction (70-80 %) of the pump radiation to be absorbed in a single pass through a 14 period active region.

We have recently reported on a high-power W-IA design with low optical confinement [2]; that laser operated with a spectral output near 3.8 μm, a peak optical power of 5 W (T = 84 K), and a power conversion efficiency of 18%. In our latest W-IA designs, we have observed considerable improvements in power extraction attributable to increasing the number of W quantum wells in the active region and pumping a larger gain-length cavity. For example, for the 3.4 μm laser reported on here, a peak optical power of 11.5 W and a power conversion efficiency of 21.2% were obtained for a 4 mm-long device operated at 84 K.[4] Certainly, the high brightness of these W-IA lasers make them suitable candidates for a number of demanding military and civilian applications, including IR countermeasures and remote sensing in the light detection and ranging (LIDAR) mode.

One of the operational drawbacks of the W-IA and other similar type-II W laser designs is their low thermal tolerance.[1-5] This is manifested by low T_0 values and by a

rapidly decreasing power slope efficiency as the device temperature is elevated. A number of theories have been advanced to explain the poor thermal performance, including inter-valence band absorbance (IVBA)[5,6] and Auger recombination.[7] IVBA is typically associated with a rapidly increasing internal loss that occurs with increasing temperature. For example, in a report on an optically pumped 4 μm GaInSb/InAs/AlSb multiple quantum well laser, the internal loss coefficient was observed to increase from 18 cm^{-1} near 70 K to 60-100 cm^{-1} near 180 K, while the internal efficiency, η_{int}, remained constant.[5] Similarly, in the work of Bewley et. al.[6] the internal loss was observed to increase from 11-14 cm^{-1} at 100 K to 50-120 cm^{-1} at 200 K for an optically pumped type-II laser with InAs/GaSb/$Ga_{1-x}In_xSb$/GaSb superlattice active region emitting near 3 μm. In contrast to these results is the work of Suchalkin et. al., who investigated the internal loss in a 3 μm W quantum well diode laser with an AlGaAsSb/InAs/InGaSb/InAs superlattice active region; they reported no increase in the internal loss of ~ 19 cm^{-1} as the temperature was elevated from 80 to 160 K.[7] They concluded that the main contribution to the waveguide loss was due to waveguide/cladding loss rather than IVBA and that the poor T_0 performance was due to Auger recombination.

In this paper, we report on measurements of the temperature dependence of the gain and internal waveguide loss of a 3.4 μm, optically pumped, type II, W-IA laser. A high-resolution FTIR spectrometer was used to measure the laser mode spectra below threshold. Our results indicate very low loss ($a \approx 2$ cm^{-1}) at 78 K, with no apparent increase up to at least 120 K. Further, measurements of the peak gain at constant pumping show a rapid decline with increasing temperature. Theoretical empirical pseudopotential model (EPM) based calculations suggest that the large differences

between the conduction and valence subband in-plane curvatures contribute substantially to the rapid decline in gain.

Experimental

The lasers were grown in our laboratory using a commercial solid-source MBE system, configured specifically for antimonide alloy deposition. Details of the eptixial growth have previously been described.[2] However, in the present design the laser structures incorporate fourteen type-II quantum wells instead of 10, as formerly used. Each type-II well is comprised of a ~ 24 A thick $In_{0.4}Ga_{0.6}Sb$ hole bearing layer, which is sandwiched in between two ~ 12 A thick coupled InAs electron wells.

Hakki-Paoli measurements of subthreshold gain and internal waveguide loss were made using a Nicolet Magna 760 FTIR spectrometer at 0.125 cm^{-1} resolution, with boxcar apodization. For mid-IR laser spectroscopy, FTIR spectrometers are ideal subthreshold measurement instruments, due to their high spectral resolution, as well as their ability to collect and average multiple spectra, thereby dramatically increasing the signal to noise ratios. To properly configure the instrument, the white light source was removed, and the output of the laser was sent along the source optical path, through the aperture that is normally used by the white light source in the spectrometer. The complications associated with multiple lateral mode effects, as well as transverse waveguide effects, were significantly reduced by passing the laser radiation through a 0.5mm slit spatial filter before it entered the FTIR. This lateral far-field filtering provides a nearly single lateral mode input.[8]

The 1.5mm x 3mm laser chip was mounted epi-side up on a copper heat sink, using indium solder, and placed in LN2 cryostat. After cryogenic cooling, the device was pumped with a low power 1.84 μm laser diode array. The pump light illuminated a ~ 226 μm wide stripe that traversed the 1.5mm long laser cavity. The pump radiation into the device is attenuated, due to Fresnel reflections at the dewar window and chip surface. Additionally, we estimate that between 75% to 85% of the radiation transmitted into the chip is absorbed in the integrated absorber/active layers. Consequently, about 54% of the input radiation was used to pump the device. A schematic of the experiment is given in Figure 1.

The single-pass power gain of the device, G, is given by exp(g-a)L, where g is the intensity gain per unit length, or the small signal gain, and a is the internal loss coefficient. The gain, G, can be determined from the following function for the spectral output (S) of a Fabry-Perot cavity:

$$S = \frac{C}{\left(1+(RG)^2 - 2RG\cos\delta\right)} \quad . \tag{1}$$

Here, R represents the modal facet power reflectivity, $\delta = 4\pi\bar{n}L/\lambda$, where $\bar{n}$ is the modal index, L is the device length, λ is the device wavelength and C is an amplitude-scaling factor. This derivation assumes a single lateral and transverse mode propagating between the facets, with $RG = 1$ corresponding to the laser threshold. It also neglects any incoherent scattering phenomena that might occur in the laser media or at the facet mirrors. Often, the device gain is obtained by determining the maximum (peaks) and minimum (valleys) of the spectra.[8,9] In Eq. (1), these minima and maxima correspond to frequencies where cos(δ) = (+/- 1). By determining the ratio of these peak and valley

values, Eq. (1) can be easily manipulated to find G. However, we note that if the subthreshold Fabry-Perot spectrum rides on top of an incoherent background, this peak-to-valley fitting procedure leads to a systematic error in G, such that G is underestimated.

In order to obtain a more accurate determination of the gain, we do not use the peak-to-valley ratio method, but rather employ a full curve fit to the spectral data, using Eq. (1) and modifying it to allow for the presence of an incoherent background:

$$S = \frac{C}{\left(1 + (RG)^2 - 2RG\cos\delta\right)} + \eta. \qquad (2)$$

The fit parameters include C, RG, δ and a dc offset term, η, that accounts for any background. The full curve fit procedure is most important when good lateral mode filtering cannot be employed, due to FTIR signal–to-noise limitations. In this case, it is preferable to use equation 2 since the full-fit can still yield accurate G values, whereas use of the peak-to-valley method will be compromised with the error increasing with increasing η. We found that the best balance between signal and background levels occurred when we used modest spatial filtering. This modest spatial filtering, coupled with a full curve to the data, helps ensure accurate determinations of G.

At energies below the band-gap, there are relatively few radiative upper and lower states and, as such, the small signal gain approaches zero ($g \sim 0$). Consequently, at these energies in the bandgap, where the RG products are small, the internal loss can be determined from:[7]

$$a \approx -\ln(G)/L. \qquad (3)$$

Equation 3 will give an accurate value for the waveguide loss if a full-curve fit, including a background term, is used. However, we note that if good lateral mode filtering is employed the waveguide loss numbers determined via full curve fit and those determined via the peak-to-valley method are comparable.

Results/Discussion

Figure 2a shows a section of a typical subthreshold gain spectrum recorded at 78.5 K and at a pumping fluence of 156W cm^{-2}. For clarity, only a portion of the low-energy side of the spectrum is shown. Fabry-Perot modulations were observed to extend from approximately 3.322μm (0.3733 eV) to 3.697μm (0.3355 eV) for a full width of ~ 38 meV. Lasing occurred at a pump intensity of 178 W cm^{-2} at $\lambda = 3.437$ μm (0.3609 meV). This indicates that emission occurs ~ 25 meV below and ~ 12 meV above the lasing energy.

A magnified view of two of the longitudinal modes from the gain spectrum of Fig. (2a) is shown in Fig. (2b). The solid line gives the results of a full curve fit to the data, using Eq. (3). A nonlinear least-squares algorithm was used to solve for the coefficients.[10]

Starting values for the *RG* and δ coefficients were determined by calculating the etalon finesse from the mode width and the phase shift from the locations of the peak maxima, respectively. From the *RG* seed value, the starting point for the scaling factor, *C*, could also be estimated. These starting coefficients typically resulted in rapid convergence, and yielded the excellent fit shown in Fig. (2b). The *RG* product, determined from this fit, was 0.29. This two-mode fitting procedure was shifted over the

entire gain spectrum, and the curves shown in Fig. (3), which plots the *RG* product vs. energy, were obtained.

Figure (3a) shows *RG* data collected at 78 K and at three different pumping levels. Note that the peak of the gain is blue-shifted as the pumping is increased and may be attributable to band filling. Also, as has been observed in other Hakki-Paoli gain/loss studies[7], all the curves converge on the low energy side of the gain spectrum where $g \sim 0$. For $E \leq 0.350$ eV, $RG \approx 0.24$. Using the mirror reflectivity, *R*, of 0.342 and Eq. (3) a very low internal wavequide loss of 2 cm^{-1} is calculated. Similarly, the gain data collected at 120 K shows convergence of the *RG* products ($RG \approx 0.29$) for $E \leq 0.341$, which yields a slightly lower waveguide loss of 1.0 cm^{-1}. These results indicate that, at least over this temperature range, IVBA is not a significant thermal degradation mechanism in contrast to previously reported results.[5,6]

It is of interest to compare these loss numbers with ones obtained by the more common method of cleaving different cavity length lasers and measuring the differential quantum efficiency (DQE) as a function of cavity length

$$\eta_d^{-1} = \eta_i^{-1} \left[\frac{2 L a}{-\ln (R_f R_b)} + 1 \right] , \qquad (4)$$

in which η_i is the internal efficiency. Using this method we find losses of 1.5 cm^{-1} and 0.13 cm^{-1} for temperatures of 90 K and 120 K, respectively; this is consistent with the low losses reported from the gain measurements. However, due to the observation that substrate modes can run in these lasers and that they can affect the DQE measurement, we believe that the losses determined from the gain measurement are more reliable. [11]

Figure (4) plots the DQE as a function of temperature for a 1.5 mm cavity length laser. The double-ended quantum efficiency, η_d, approaches 0.7 at cryogenic temperatures. However, a rapid, nonlinear, decrease in the DQE occurs when the temperature is increased. At 120 K, the DQE has been reduced to ~ 0.44. Using Eq. (4) and the measured a and η_d the laser internal efficiency may be determined. Internal efficiencies of 0.85 and 0.57 were calculated for T = 90 K and 120 K, respectively. In comparison, the η_i determined from the DQE vs. cavity length measurements gave 0.83 and 0.5 at these temperatures. These results suggest that for the W-IA laser structure the decrease in the internal laser efficiency is a significant factor limiting the thermal performance of these devices.

To obtain a more detailed understanding of the modal gain properties of the device and to assist in understanding the origin of the rapidly declining internal efficiency with increasing temperature, two additional laser gain measurements were performed. In the first experiment, the laser gain was measured as a function of pump power. This was repeated for several different temperatures. In the second, the peak laser gain was measured as a function of temperature at a fixed pumping power. Figure 5 shows the results of the first experiment and plots the gain vs. absorbed pump power at four temperatures. It is clear that the pumping required to reach a particular gain value increases dramatically with temperature. For example, Figure 6 (right y-axis) plots the pump power required to reach device transparency, $g = a$, as the temperature is increased. We note that the dependence is well-fit by an exponential function given by the solid line, and that the transparency pump power increases approximately by a factor of four for every 50 degree K increase in temperature. Further, the figure also indicates that the

differential gain, dG/dP, evaluated in the interval from g = 0 to g = 4, has a strong temperature dependence. This can also be seen in Figure 6 (left y-axis) which plots the differential gain as a function of temperature; the differential gain drops by a factor of approximately two when the temperature is increased from 78 K to 100 K.

Finally, Figure 7 shows the results of the experiment in which the pump power was fixed at 865 mW and the temperature increased from 100 to 130 K. A rapid linear fall-off in the peak gain is seen as the temperature is raised.

Interestingly, gain calculations, based on our superlattice empirical pseudopotential method (SEPM), correlate well with the observations displayed in Figure 5. A description of those calculations follows: For several years now, we have advocated pseudopotential approaches as more accurate alternatives to envelope function methods for calculating the electronic and optical properties of Type-II mid-IR lasers.[12,13] Our SEPM requires an empirical pseudopotential description of the bulk component materials, and then, using only the energy-band lineups or offsets between component materials, fuses the bulk-like layer potentials into the pseudopotential for the superlattice. In the SEPM, we make the critical assumption that the heterointerface charges redistribute, forming charge and dipole sheets near the interface, in order that the layer pseudopotentials remain as bulk-like as possible. This leads to a considerable reduction in parameters when compared to other methods. (See Reference 13 for a detailed comparison of pseudopotential methods for superlattices.)

We make our gain calculations by first using the SEPM to calculate the subband energies for the superlattice active region. In particular, we calculate energies for the two lowest conduction subbands, as well as the highest four valence subbands. Once these

subband energies are stored as functions of the Bloch momenta defining the in-plane phase space for the superlattice, we calculate the gain as an integration over all of the direct transitions from occupied states in the lowest conduction subbands to empty states in the top valence subbands. In addition, each electron to hole transition is homogeneously broadened with a Lorentzian lineshape, in which the Lorentzian width is set at 3 meV. For each case, we fix the Fermi levels to ensure equal electron and hole sheet densities per period of the active region superlattice.

These fixed inversion results with the areal density at 6.08×10^{12} cm $^{-2}$ are plotted as a function of energy in figure 3a for T = 78 K. We note reasonable agreement with the gain data plotted as a function of energy. In a second calculation, we isolated on the fixed inversion peak gain value, g, as a function of temperature. These results are shown in the upper curve of figure 7. The results show a forty percent reduction in the gain as the temperature increases from 100 K to 130 K. We attribute this type of gain reduction to the large differences between the valence and conduction subband curvatures that naturally exist in this W laser structure. In particular, the flatter valence subbands allow the holes to spread significantly in the in-plane phase-space, so that the number of directly radiatively connected electrons and holes are reduced. This fixed inversion gain reduction is independent of nonradiative recombinations such as Auger and Shockley-Reed. The lower theory curve in figure 7 matches the measured gain reduction. This curve was generated by decreasing the inversion at each temperature until theory matched experiment. We estimate that a modest inversion reduction from to 6.08×10^{12} per cm^{-2} to 5.01×10^{12} cm $^{-2}$ will account for the observations.

Conclusions

The gain and loss properties of a 3.4 μm optically pumped InAs/InGaSb, W-integrated absorber laser were studied by employing an FTIR spectrometer to record the subthreshold gain spectra. In order to obtain a more accurate assessment of the gain, a full curve fit to the mode spectrum was used that included a "DC offset" correction to account for the presence of an incoherent background. The full curve fit procedure is most important when good lateral mode filtering cannot be employed, due to FTIR signal–to-noise limitations

Of particular interest are the G values determined on the low-energy side of the spectrum, below the band gap energy, where the small signal gain is near zero.[7] These sub-band gap G values may be used to determine the waveguide loss. Using this method, we measured very low optical losses of $a = 2$ cm^{-1} at 78 K. Higher values of loss have been reported for W lasers where the Hakki-Paoli peak-to-valley method was used in determing the gain.[7] We note that without good lateral mode filtering the Hakki-Paoli peak-to-valley method can substantially underestimate the device gain. Here we obtained good accuracy by employing a full spectral curve fit, as well as a lateral mode filter.

No increase in the loss was observed when the temperature was increased to 120 K; this indicates negligable IVBA activation with increasing temperature. This result stands in contrast to previous observations on mid-IR W lasers that showed dramatic increases in the internal loss and IVBA with increasing temperature.[5,6]

Determination of the internal laser efficiency, η_i, from the measured differential quantum efficiency and a suggests that a rapid decline in the η_i with temperature is the primary reason for the limited temperature operation range of these lasers.

Measurements of the gain as a function of pumping show a rapid fall-off in the differential gain with temperature. In a similar vein, measurements of the peak gain at fixed inversion show a rapid linear decrease as the temperature is raised. Gain calculations based on the superlattice empirical pseudopotential method accurately predict this behavior and indicate that ~ 40 % of the gain decline is due to the large differences between the valence and conduction subband curvatures that naturally exist in this W structure. This fixed inversion gain reduction is independent of nonradiative recombinations such as Auger and Schockley-Read. The remaining decline in the gain can be accounted for by assuming a relatively small decrease < 20 % in the initial carrier density. This depletion in the carriers may be due to nonradiative processes such as Auger recombination or carrier detrapping, particularly hole escape, from the wells.

References

1. A. K. Goyal, G. W. Turner, H. K. Choi, P. J. Foti, M. J. Manfra, T. Y. Fan, and A. Sanchez, Lasers and Electro-Optics Society (LEOS) Annual Meeting, Puerto Rico, 2000, p. 249.
2. R. Kaspi, A. P. Ongstad, G. C. Dente, J. Chavez, M. L. Tilton, and D. Gianardi, Appl. Phys. Lett., 81(13), 406, (2002).
3. A. P. Ongstad, R. Kaspi, J. R. Chavez, G. C. Dente, M. L. Tilton, and D. M. Gianardi, J. Appl. Phys., 92(10), 5621, (2002).
4. R. Kaspi, A. P. Ongstad, J. R. Chavez, G. C. Dente, M. L. Tilton, and D. M. Gianardi, in preparation, (2003).
5. H.Q. Le, C. H. Lin, S. J. Murray, R. Q. Yang and S. S. Pei, I.E.E.E. J. Quant. Electron., 34(6), 1016, (1998).
6. W. W. Bewley, I. Vurgaftman, C. L. Felix, J. R. Meyer, C. H. Lin, D. Shang, S. J. Murry, S. S. Pei, and L. R. Ram-Mohan, J. Appl. Phys., 83(5), 2384, (1998).
7. S. Suchalin, D. Westerfeld, D. Donetsik, S. Luryi, G. Belenky, R. Martinelli, I. Vurgaftman, and J. Meyer, Appl. Phys. Lett., 80(16), 2833, (2002).
8. J. Stohs, D. J. Bossert, D. J. Gallant, and S. R. J. Brueck, I.E.E.E. J. Quant. Electron., 37(11), 1449, (2001).
9. B. W. Hakki and T. L. Paoli, J. Appl. Phys, 46(3), 1299, (1975).
10. W. H. Press, "Numerical Recipies in C: The Art of Scientific Computing", Cambridge Univ. Press, Cambridge England, 1988.

11. M. L Tilton, G. C. Dente, A. P. Ongstad, R. Kaspi, J. Chavez, and D. Gianardi, 5th International Conference on Mid-IR Optoelectronic Materials and Devices (MIOMD-V), Annapolis, Md., 2002, p. 165.

12. G. C. Dente and M. L. Tilton, J. Appl. Phys., 86, 1420, (1999).

13. G. C. Dente and M. L. Tilton, Phys. Rev. B., 66, 165307, (2002).

Figure Captions

Figure 1. Diagram of the optical pumping experiment used to measure the gain/loss properties of the mid-IR laser.

Figure 2a. Section of a subthreshold gain spectrum showing a portion of the low energy side. The spectrum was collected at T = 78.5 K, and I = 156 W cm^{-2}. The peak of the gain was near 0.3610 eV (3.436 um). 2b. A full curve fit, using equation 3, to the two modes indicated in figure 1a. □ - experimental data.

Figure 3. Spectral dependence of the gain. Top panel: T = 78 K, L = 1.5 mm, P_{abs} = 0.28, 0.37 and 0.53 watts. The solid line gives the theory fit to the P_{abs} = 0.53 W data and used a = 1.5 cm^{-1}, Δ = 2 meV. Bottom panel: T = 120 K, L = 1.5 mm, P_{abs} = 0.74, 1.01, 1.14 watts.

Figure 4. A plot of the differential quantum efficiency vs. temperature. The plot shows data for a L = 1.5 mm laser.

Figure 5. A plot of the small signal gain, g, vs. pump power at four different temperatures.

Figure 6. A plot of the: differential gain vs. temperature (left y-axis) and a plot of the pumping power required to reach device transperancy vs. temperature (right y-axis).

Figure 7. A plot of the peak gain vs. temperature for a fixed pumping power of 865 mW. ● - experimental data, dash-dot - SEPM theory with fixed inversion, dash – SEPM theory with varying inversion.

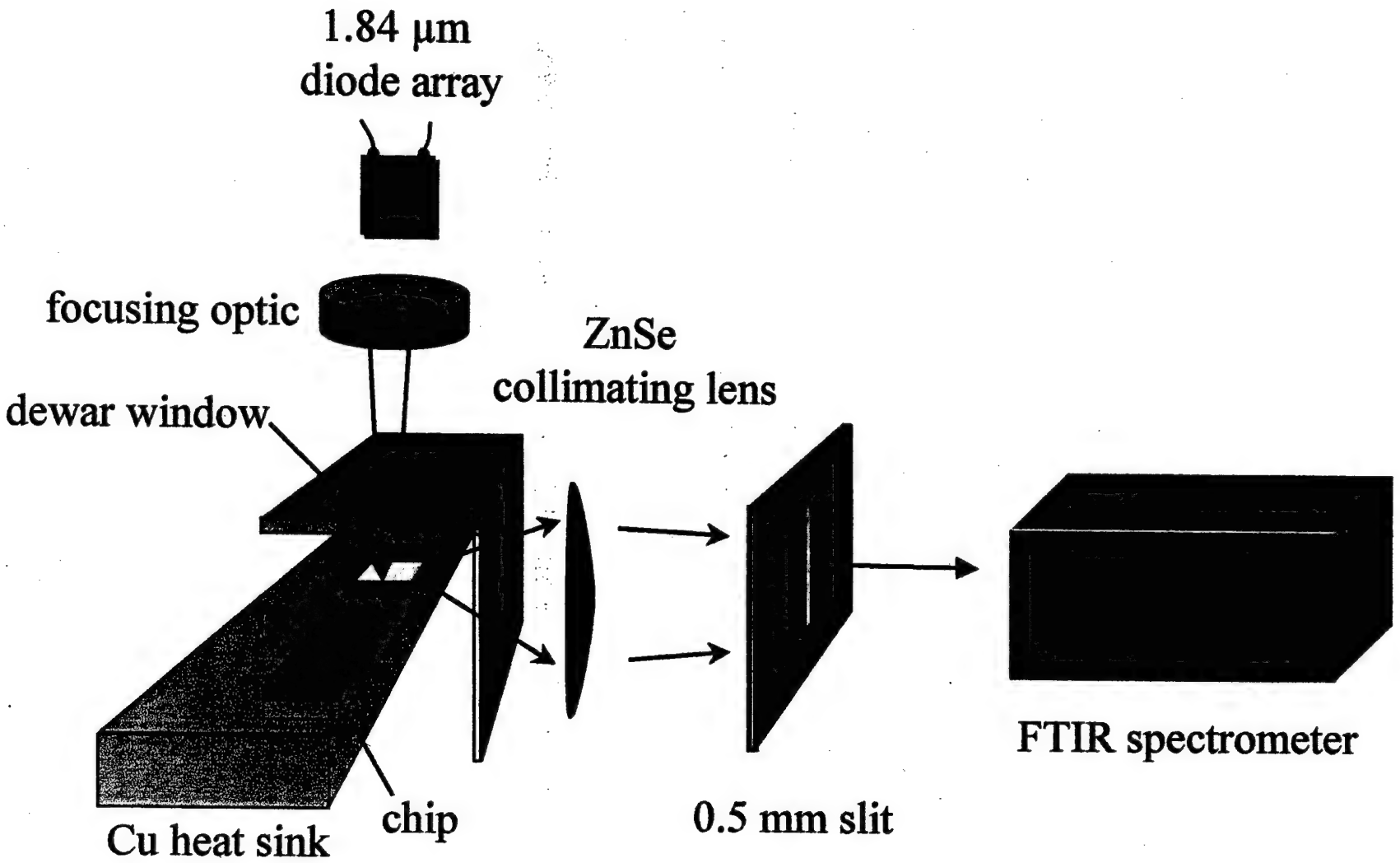

Figure 1, Ongstad et. al.

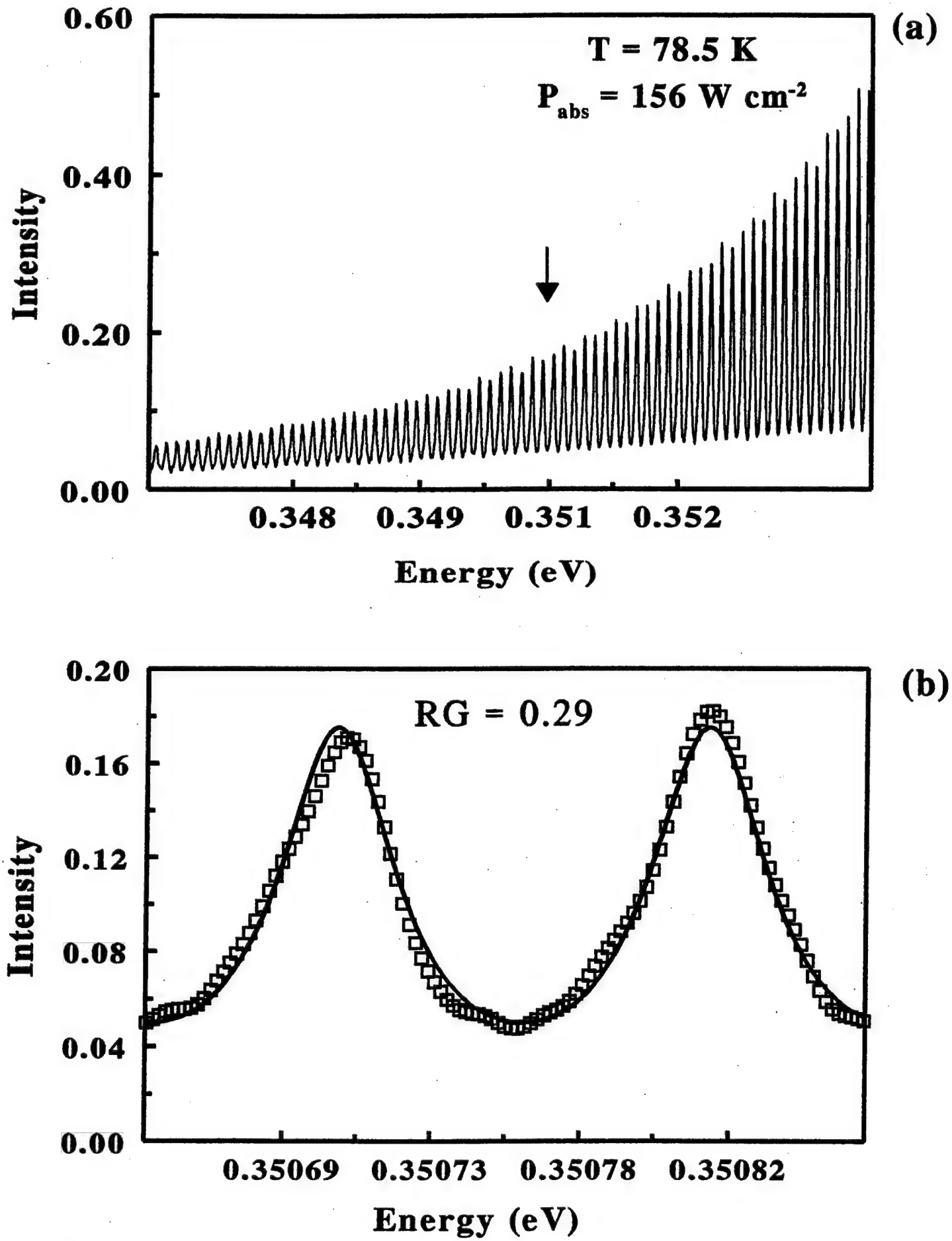

Fig. 2, Ongstad, et.al.

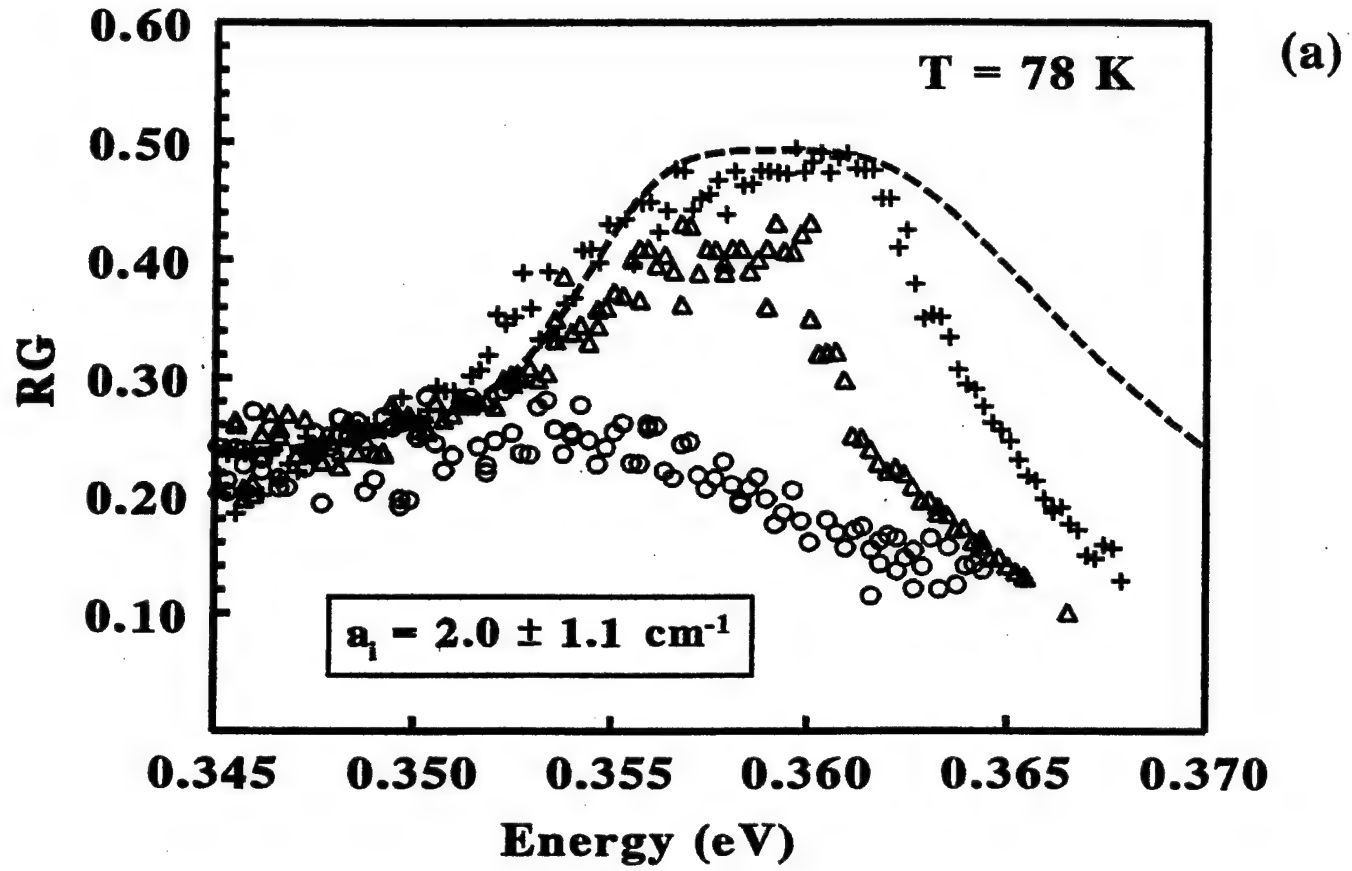

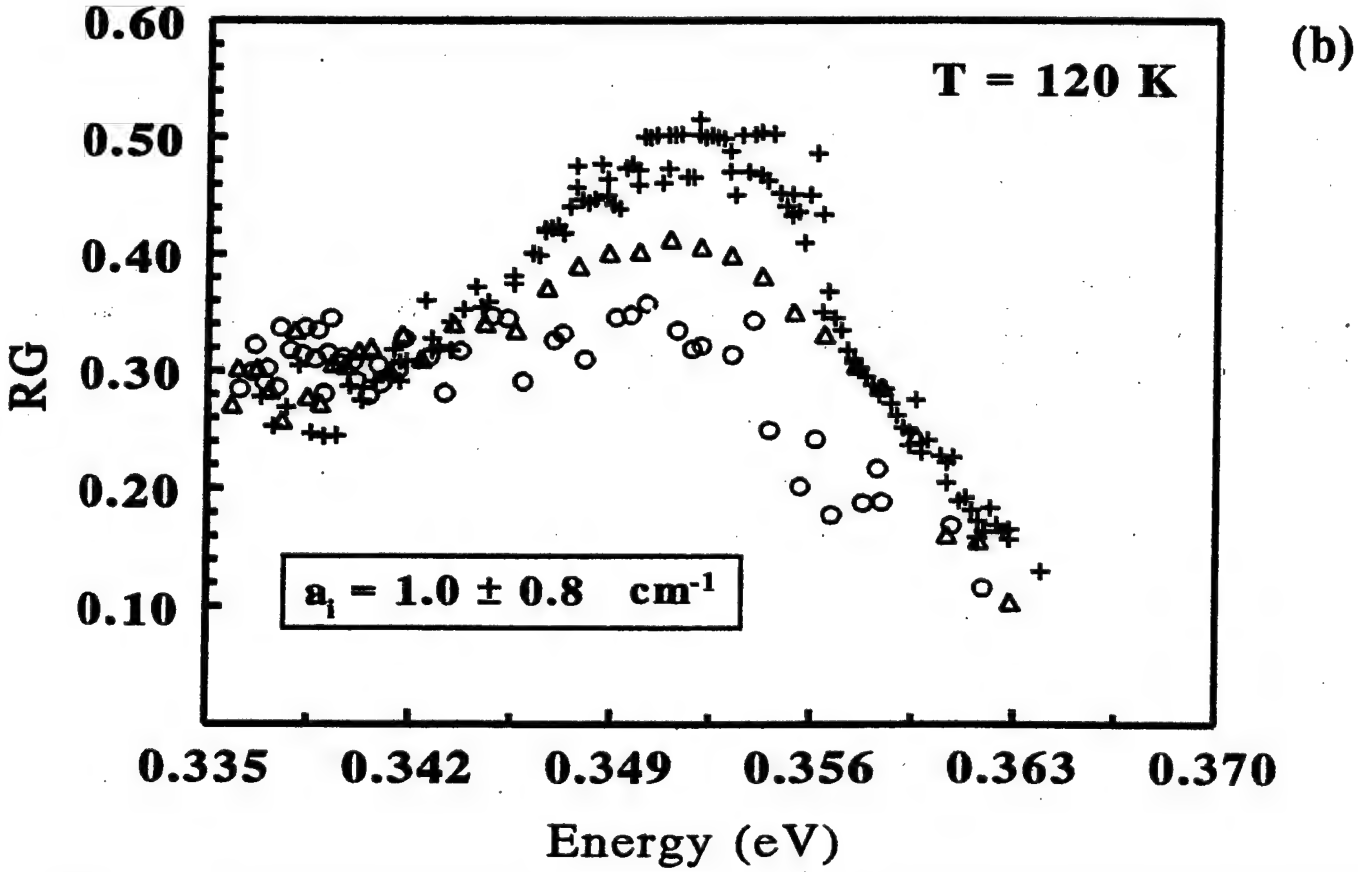

Fig. 3, Ongstad, et.al.

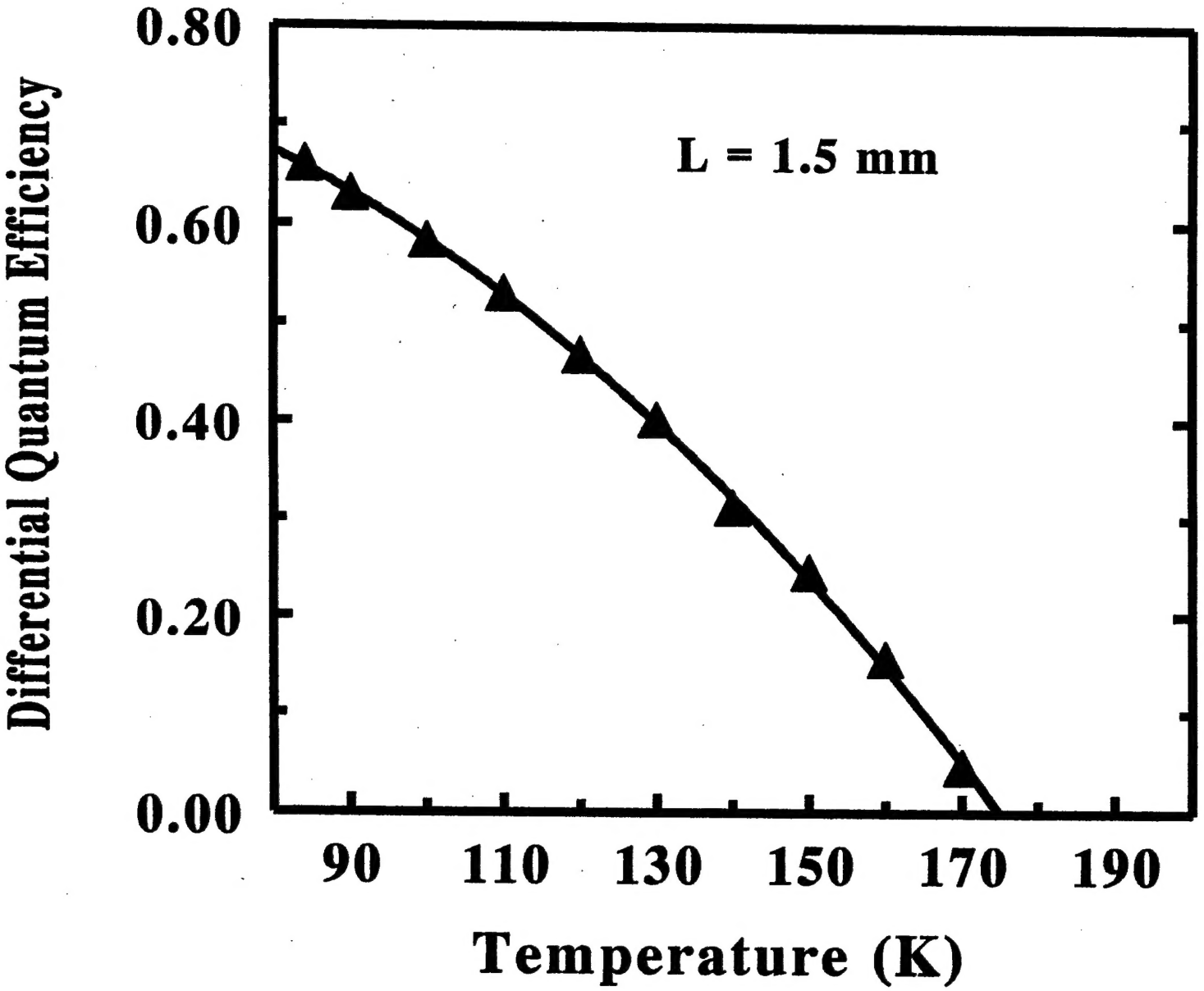

Fig. 4, Ongstad, et.al.

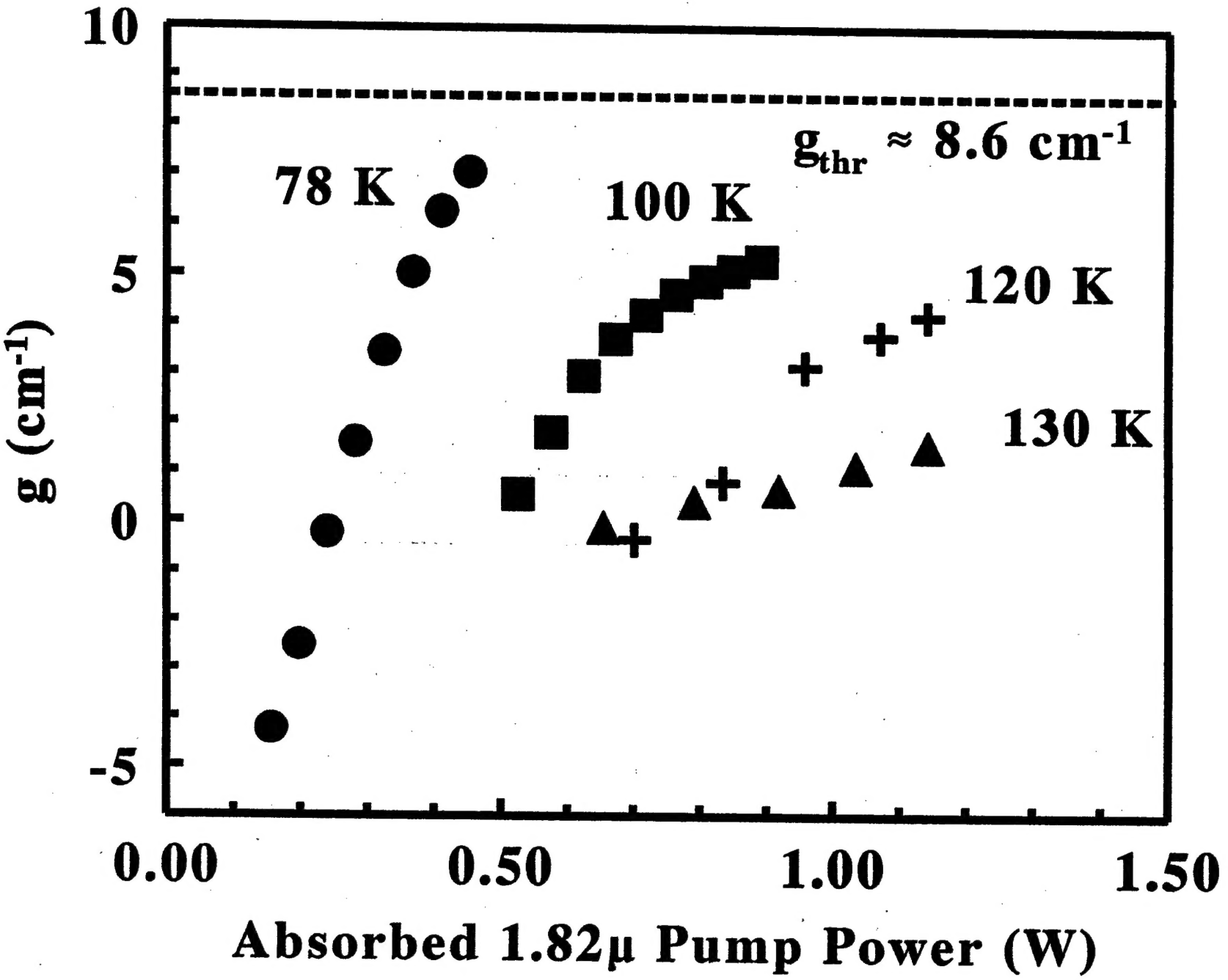

Fig. 5, Ongstad, et.al.

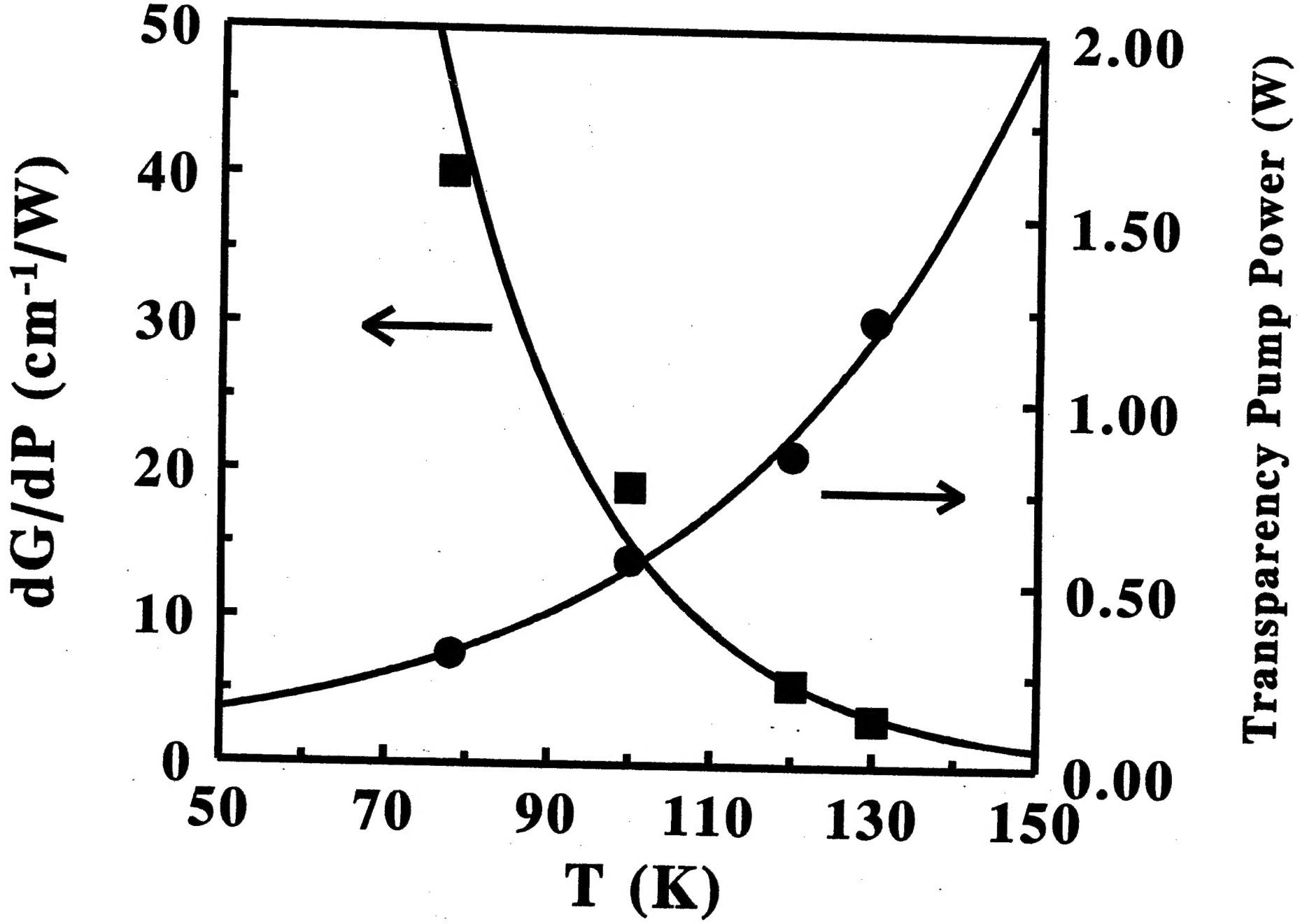

Figure 6, Ongstad et. al.

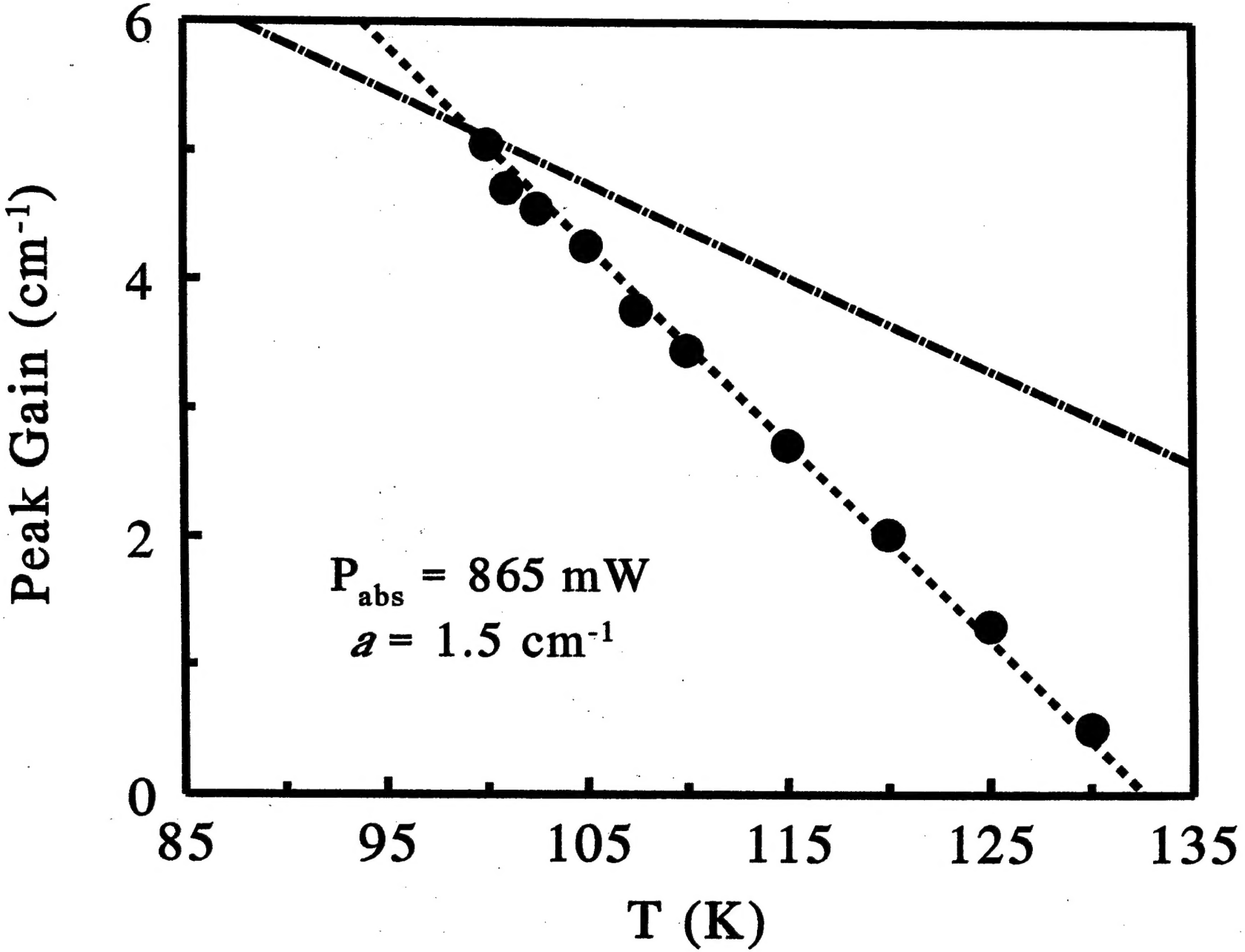

Fig. 7, Ongstad, et.al.